Adaptive Fuzzy Iterative Learning Control of Constrained Systems With Arbitrary Initial State Errors and Unknown Control Gain

Huihui Shi, Qiang Chen, *Member, IEEE*, Yihuang Hong, Xianhua Ou, *Member, IEEE*, and Xiongxiong He

***Abstract*— An adaptive fuzzy iterative learning control(AFILC) method is presented to address the state tracking issue of constrained systems with arbitrary initial state errors and unknown control gain. A novel desired error trajectory is systematically developed in the polynomial form to relax the identical initial condition, which allows for arbitrary setting of initial values for all the system state errors. The proposed desired error trajectory can also relax the iteration-invariance restriction on the reference signals due to the independence of the reference trajectories. An asymmetric integral fractional barrier Lyapunov function is developed, keeping the tracking error within the preassigned boundary. Moreover, there is no need to estimate the unknown control gain function in the controller design, reducing computation burden. Numerical simulations and experiments in the permanent magnet synchronous motor experimental platform are provided to illustrate the efficacy of the proposed method.**

***Note to Practitioners*—Most practical systems often perform repetitive tasks in industrial processes, such as the repetitive handling process of manipulators, and the rotation process of motors, etc. Iterative learning control method is model independent, and fully utilizes the repetitive characteristics during system operation. However, due to irregular initial state drifts caused by locating operations at different iterations, the identical initial condition is often violated in practical iterative learning control applications. This paper presents an adaptive fuzzy iterative learning control method to address the state tracking issue of constrained systems with arbitrary initial state errors and unknown control gain. The problem of inconsistent initial values is addressed by designing a desired error trajectory in the polynomial form, such that arbitrary setting of initial values for all the system state errors is allowed. For safe operation in practice, an asymmetric integral fractional barrier Lyapunov function is developed to keep the tracking error within the preassigned boundary. The satisfactory experimental results on the permanent magnet synchronous motor experimental platform also demonstrate the practical effectiveness of the proposed method.**

Manuscript received 23 June 2024; accepted 8 August 2024. This article was recommended for publication by Associate Editor Q. Zhu and Editor C. Seatzu upon evaluation of the reviewers' comments. This work was supported in part by the National Natural Science Foundation of China under Grant 62222315, Grant 62303418, Grant 61973274, and Grant 62233016; and in part by Zhejiang Provincial Natural Science Foundation of China under Grant LZ22F030007. *(Corresponding author: Qiang Chen.)*

The authors are with the Data-Driven Intelligent Systems Laboratory, College of Information Engineering, Zhejiang University of Technology, Hangzhou, Zhejiang 310023, China (e-mail: shidemelei@163.com; sdnjchq@zjut.edu.cn; 211122030123@zjut.edu.cn; xhou@zjut.edu.cn; hxx@zjut.edu.cn).

Color versions of one or more figures in this article are available at https://doi.org/10.1109/TASE.2024.3445670.

Digital Object Identifier 10.1109/TASE.2024.3445670

***Index Terms*— Adaptive fuzzy iterative learning control, integral barrier Lyapunov function, desired error trajectory, unknown control gain.**

I. Introduction

ITERATIVE learning control (ILC) is able to provide complete tracking performance in repeating operations within a limited time interval [1], [2], [3], [4]. Based on the Lyapunov theorem, a parametric learning method, adaptive iterative learning control (AILC) is developed, and the error information in precious cycles is employed to update the estimation of parameters, which broadens the application scope of the ILC methods [5], [6], [7]. In the learning process, some essential fundamental assumptions, such as the identical initial condition and consistent reference signal, are usually required to be met in each iteration [8]. However, the reference signals in each iteration are hardly consistent in practical industrial operations with unpredictable factors. The inconsistency of the reference signals may cause the learning process to restart. To relax the iteration-invariance restrictions on the reference signals, some research efforts have been undertaken to address the issues of ILC and AILC design with iteration-varying reference signals [9], [10], [11].

On the other hand, due to irregular initial state drifts caused by locating operations at different iterations, the identical initial condition is often violated in practical ILC and AILC applications. Consequently, various methods have been presented for relaxing such restriction, including time-varying boundary layer method [12], [13], initial rectifying method [14], [15], alignment conditions [16], [17], error-tracking method [18], [19], [20] and so on. The initial rectifying method constructs a transition trajectory to correct the reference signal, such that the initial condition is consistent. However, the rectified trajectory should be redesigned in each iteration as tracking iteration-varying reference signals, which may increase the amount of computation. An error-tracking ILC was first proposed in [18], and a desired error trajectory was formed to avoid the repeated construction of rectified trajectories. In [19] and [20], different error tracking AILC schemes were respectively proposed for output or state tracking of nonlinear systems with initial shifts. In the previous work [18], [20], [21], the first initial state error is allowed to be set arbitrarily, while the other initial values of state errors are assumed to be zero for constructing the desired error trajectories. Consequently, it motivates us to design an effective AILC scheme to handle the state tracking issue with arbitrary initial state errors.

Moreover, constraints are usually imposed on the system inputs and outputs to ensure the operation security in practice, such as input dead-zone, input saturation and so on [22], [23], [24], [25], and [26]. In order to address input constraint control problem, intelligent approximation tools like fuzzy logic systems [27], [28], [29], [30] and neural networks [31], [32], [33] are widely employed. Reference [34] utilized the fuzzy logic systems and adaptive compensation approach to approximate the system nonlinearities, and the processing difficulty of the unknown nonlinearities is reduced. Except for input constraints, it has practical significance to cope with the output constrained control issues because many practical systems are subject to various performance limitations in the working process [35], [36], [37], for instance, the operating speed of the high-speed trains should be constrained to prevent the trains from over speed. Various effective control approaches have been proposed to avoid violating constraints, such as funnel control [38], [39], [40], prescribed performance control [41], [42], [43], [44] and so on. As an alternative, barrier Lyapunov function (BLF) is developed based on the Lyapunov theory, which does not require designing new error variables [45], [46], [47], [48], [49]. Under the iterative learning control framework, BLFs in logarithm and tangent forms are often employed to avoid violating system output constraints in each iteration [50]. Compared with symmetric constraints, the asymmetric constraints may be more common in practical requirements [51], [52], [53], [54], [55]. However, in the construction of asymmetric BLFs, the discontinuity is avoided by raising the error variables to the high power, which may result in high-gain control signals for large error value at the beginning. In [56], an asymmetric barrier function was constructed for nonlinear systems with partially known control gains. The upper bounds of control gain functions were estimated by designing parametric ILC update laws, which would increase the computational burden.

Referring to the above observation, an adaptive fuzzy iterative learning control scheme is proposed for constrained systems with arbitrary initial state errors and unknown control gain. Through constructing a desired error trajectory to avoid assumptions of the initial state values and reference trajectory. Then, an asymmetric integral fractional barrier Lyapunov function (AIFBLF) is designed. A fuzzy logic system is employed in the controller design to approximate system uncertainties, and the combined adaptive learning laws are developed to restrain the ceaseless positive accumulation issue by using the leakage terms. The contributions of this article are as follows.

1) A novel desired error trajectory is systematically constructed in the polynomial form, such that the restrictions on the initial state values and reference signals are relaxed. Compared with the previous work [18], [19], [20], [21] that only considering the arbitrary first initial state output error, in this paper, the desired error trajectory includes all the system state errors to handle the initial state inconsistency problem.

2) Compared to the traditional ABLFs [52], [53], [54], an asymmetric integral fractional barrier Lyapunov function is presented to constrain system tracking error within the preassigned boundary, and high-gain control signals for large error value at the beginning is avoided. In addition, low computational burden is achieved due to the avoidance of estimating the upper bound of unknown control gain function.

The reminder of this paper is provided as follows. Section II gives the constrained nonlinear system and preliminaries. A desired error trajectory for a class of nth-order constrained systems is constructed in Section III. The adaptive fuzzy iterative learning controller and asymmetric integral fractional barrier Lyapunov function are designed in Section IV. The tracking error convergence analysis is provided in Section V. Section VI shows the results of simulation and experiment. The conclusions are given in Sections VII, respectively.

II. Problem Formulation and Preliminaries

A. System Description

The nth-order constrained system is described by

$$\begin{cases} \dot{x}_{i,k} = x_{i+1,k}, i = 1, \cdots, n-1 \\ \dot{x}_{n,k} = f(\boldsymbol{x_k}) + g(\boldsymbol{x_k})\psi(u_k), \end{cases} \tag{1}$$

where $f(\boldsymbol{x_k})$ and $g(\boldsymbol{x_k})$ denote the smooth functions of system dynamics and positive control gain, which are bounded but unknown, respectively. $\boldsymbol{x_k} = [x_{1,k}, x_{2,k}, \cdots, x_{n,k}]^T$, and $x_{1,k}, \cdots, x_{n,k}$ are the system states. $k \in N$ represents the iteration number. The system output is constrained by the requirement for $x_{1,k}$, i.e., $b_1 < x_{1,k} < b_2$ during $t \in [0, T]$ in each iteration, where b_1 is the negative constant smaller than the lower bound of $x_{d,k}$, and b_2 is the positive constant larger than the upper bound of $x_{d,k}$, and $x_{d,k}$ is the iteration-varying continuous and nth-order differentiable reference trajectory. $u_k(t)$ is the actual control input, $\psi(u_k)$ presents the input constraints,

$$\psi(u_k) = \iota(t)u_k(t) + o(t), \tag{2}$$

where $\iota(t) \in R$ is an unknown continuous function satisfying $0 < \iota_{\min} \leq \iota(t) \leq \iota_{\max}$. $o(t) \in R$ denotes a redundant function, satisfying $0 < |o(t)| \leq o_m$. $\iota_{\min}$, $\iota_{\max}$ and o_m are unknown positive boundary constants.

Define $e_{i,k}$ and $e_{n,k}$ as

$$e_{i,k} = x_{i,k} - x_{d,k}^{(i-1)}, e_{n,k} = x_{n,k} - x_{d,k}^{(n-1)}. \tag{3}$$

From (1)-(3), we have

$$\begin{cases} \dot{e}_{i,k} = e_{i+1,k} \\ \dot{e}_{n,k} = f_{n,k} + g_{n,k}(\iota(t)u_k(t) + o(t)) - x_{d,k}^{(n)}, \end{cases} \tag{4}$$

where $f_{n,k} = f(x_k, x_{d,k}^{(n)})$, $g_{n,k} = g(x_k)$.

B. Fuzzy Logic Systems (FLSs) and Lemmas

Normal FLSs contains four basic parts, which are listed as follows. 1. The fuzzy rule base; 2. The fuzzy inference engine; 3. The fuzzifier; 4. The defuzzifier [57]. The fuzzy rule base is composed of "IF-THEN" rules:

R^j:If r_1 is F_1^j, r_i is F_i^j, $\cdots$ and r_N is F_N^j, then y is G^j.

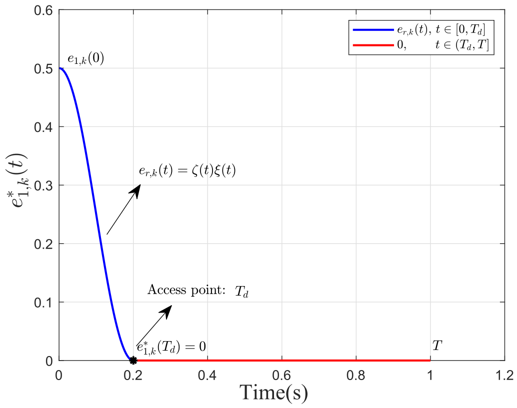

Fig. 1. The constructed desired error trajectory $e^*_{1,k}$.

where F_i^j and G^j are the fuzzy set. $r = [r_1, \cdots, r_N]^T \in R^N$ and $y \in R$ are the input and output of the FLSs, respectively. $i = 1, \cdots, N$, $j = 1, \cdots, M$, and M is the number of fuzzy inference rules.

Denote $\Psi(r) = [\varphi_1(r), \cdots, \varphi_N(r)]^T$, $W^T = [\bar{w}_1, \cdots, \bar{w}_N]^T$, and $\omega_{F_i^j}(r_i)$ and $\omega_{G_i^j}(y)$ as the fuzzy membership functions of F_i^j and G^j, respectively.

Define a fuzzy basis function as

$$\varphi_l(r) = \frac{\prod_{i=1}^{N} \omega_{F_i^j}(r_i)}{\sum_{j=1}^{M}\left[\prod_{i=1}^{N} \omega_{F_i^j}(r_i)\right]}. \tag{5}$$

Then, the output of the FLSs can be generated as

$$y(r) = \frac{\sum_{j=1}^{M} \bar{w}_j \prod_{i=1}^{N} \omega_{F_i^j}(r_i)}{\sum_{j=1}^{M}\left[\prod_{i=1}^{N} \omega_{F_i^j}(r_i)\right]} = W^T\Psi(r), \tag{6}$$

where $\bar{w}_j = \max_{y \in R} \omega_{G_i^j}(y)$.

Lemma 1 ([6]): There exist a sequence $s_k(t)$, the derivative of the sequence $\dot{s}_k$ and a positive integer k, if $\dot{s}_k$ is uniformly bounded on $[0, T]$, and the following condition holds

$$\lim_{k\to\infty} \int_0^T s_k^2(\tau)d\tau = 0 \tag{7}$$

then, on $[0, T]$, $\lim\limits_{k\to\infty} s_k(t) = 0$ uniformly.

III. Desired Error Trajectory Construction

In this section, the construction of the continuous and smooth desired error trajectory is systematically provided.

As shown in Fig. 1, design the desired error trajectories for system (1) as

$$e^*_{1,k}(t) = \begin{cases} e_{r,k}(t), & t \in [0, T_d] \\ 0, & t \in (T_d, T], \end{cases}$$
$$e^*_{i+1,k}(t) = \dot{e}^*_{i,k}(t), \tag{8}$$

where T_d is the access point, $i = 1, \cdots, n-1$. $e_{r,k}(t) = \zeta(t)\xi(t)$ is the transition trajectory, which should be smooth and $n-1$th order differentiable. The detailed construction process of the transition trajectory $e_{r,k}(t)$ is provided in the following.

The transition trajectory should satisfy the following construction conditions,

$$\begin{aligned} &e_{r,k}(0) = e_{1,k}(0), \\ &e^{(i)}_{r,k}(0) = e_{i+1,k}(0), e^{(n)}_{r,k}(0) = 0, \end{aligned} \tag{9}$$

and

$$e_{r,k}(T_d) = e^{(i)}_{r,k}(T_d) = e^{(n)}_{r,k}(T_d) = 0, \tag{10}$$

where $i = 1, \cdots, n-1$, $e_{i,k}(0)$ and $e_{n,k}(0)$ denote the initial values of $e_{i,k}(t)$ and $e_{n,k}(t)$, respectively.

According to the construction conditions (9) and (10), $\zeta(t)$ is constructed in the form of

$$\zeta(t) = e_{1,k}(0) + \sum_{i=1}^{n-1} e_{i+1,k}(0)\varsigma_i(t), \tag{11}$$

with $\varsigma_i(t)$ being a smooth function, and $\varsigma_i^{(\ell)}(0) = 0$, $\varsigma_i^{(i)}(t) = 1$, $\ell = 1, \cdots, i-1$.

Then, $\varsigma_i(t)$ is constructed as

$$\varsigma_i(t) = \frac{1}{i!}t^i. \tag{12}$$

Substituting (12) into (11), one has

$$\zeta(t) = e_{1,k}(0) + \sum_{i=1}^{n-1} \frac{1}{i!} e_{i+1,k}(0)t^i. \tag{13}$$

The function $\xi(t)$ satisfies

$$\begin{aligned} &\xi(0) = 1, \xi^{(i)}(0) = 0, \xi^{(n)}(0) = 0, \\ &\xi(T_d) = 0, \xi^{(i)}(T_d) = 0, \xi^{(n)}(T_d) = 0, \end{aligned} \tag{14}$$

From (14), the function $\xi(t)$ can be designed in the following polynomial form

$$\begin{aligned} \xi(t) = {} & a_{n+1}(1 - \frac{t}{T_d})^{2n+1} + a_n(1 - \frac{t}{T_d})^{2n} \\ & + \cdots + a_1(1 - \frac{t}{T_d})^{n+1} \end{aligned} \tag{15}$$

where $a_1, \cdots, a_{n+1}$ are positive constants to be determined later.

From (14) and (15), one can obtain

$$\begin{aligned} &\xi(0) = a_{n+1} + a_n + \cdots + a_1 = 1, \\ &\xi^{(i)}(0) = \left(\frac{(2n+1)!}{(2n+1-i)!}\frac{a_{n+1}}{T_d^i} + \frac{(2n)!}{(2n-i)!}\frac{a_n}{T_d^i} \right. \\ &\qquad \left. + \cdots + \frac{(n+1)!}{(n+1-i)!}\frac{a_1}{T_d^i}\right) = 0, \\ &\xi^{(n)}(0) = \left(\frac{(2n+1)!}{(n+1)!}\frac{a_{n+1}}{T_d^n} + \frac{(2n)!}{n!}\frac{a_n}{T_d^n} \right. \\ &\qquad \left. + \cdots + \frac{(n+1)!}{1!}\frac{a_1}{T_d^n}\right) = 0, \\ &\xi(T_d) = 0, \xi^{(i)}(T_d) = 0, \xi^{(n)}(T_d) = 0, \end{aligned} \tag{16}$$

which can be rewritten as

$$\begin{bmatrix} 1 & 1 & \cdots & 1 \\ \frac{(2n+1)!}{(2n)!} & \frac{(2n)!}{(2n-1)!} & \cdots & \frac{(n+1)!}{(n)!} \\ \vdots & \vdots & \ddots & \vdots \\ \frac{(2n+1)!}{(n+1)!} & \frac{(2n)!}{(n)!} & \cdots & \frac{(n+1)!}{1!} \end{bmatrix} \begin{bmatrix} a_{n+1} \\ a_n \\ \vdots \\ a_1 \end{bmatrix} = \begin{bmatrix} 1 \\ 0 \\ \vdots \\ 0 \end{bmatrix}. \tag{17}$$

According to the Cramer principle, there exists the unique solution for (17) given by

$$a_{n+1} = \frac{D_1}{D}, a_n = \frac{D_2}{D}, \cdots, a_1 = \frac{D_{n+1}}{D} \tag{18}$$

where $D \neq 0$ is the determinant expressed as

$$D = \begin{vmatrix} 1 & 1 & \cdots & 1 \\ \frac{(2n+1)!}{(2n)!} & \frac{(2n)!}{(2n-1)!} & \cdots & \frac{(n+1)!}{(n)!} \\ \vdots & \vdots & \ddots & \vdots \\ \frac{(2n+1)!}{(n+1)!} & \frac{(2n)!}{(n)!} & \cdots & \frac{(n+1)!}{1!} \end{vmatrix}, \tag{19}$$

and D_l, $l = 1, \cdots, n+1$, are the determinants obtained by replacing the lth column of D with the following constant vector $\mathbf{C}$, i.e.,

$$D_l = \begin{vmatrix} 1 & \cdots & 1 & \cdots & 1 \\ \frac{(2n+1)!}{(2n)!} & \cdots & 0 & \cdots & \frac{(n+1)!}{(n)!} \\ \vdots & \ddots & \vdots & \ddots & \vdots \\ \frac{(2n+1)!}{(n+1)!} & \cdots & 0 & \cdots & \frac{(n+1)!}{1!} \end{vmatrix}, \mathbf{C} = \begin{bmatrix} 1 \\ 0 \\ \vdots \\ 0 \end{bmatrix}. \tag{20}$$

From (13), (15) and (18)-(20), it is concluded that the transition trajectory $e^r_{1,k}(t)$ is constructed as

$$e_{r,k}(t) = (e_{1,k}(0) + \sum_{i=1}^{n-1} \frac{e_{i+1,k}(0)}{i!} t^i) \Bigg(\frac{D_1}{D}(1 - \frac{t}{T_d})^{2n+1} + \frac{D_2}{D}(1 - \frac{t}{T_d})^{2n} + \cdots + \frac{D_{n+1}}{D}(1 - \frac{t}{T_d})^{n+1} \Bigg). \tag{21}$$

Following (21), a systematical design method of the transition trajectory $e_{r,k}(t)$ is developed for any initial state errors $e_{i,k}(0), i = 1, \cdots, n$. For example, by using (21), for the first-order and second-order systems in the form of (1), the transition trajectories can be directly designed as

$$e_{r,k}(t) = e_{1,k}(0)\Bigg(-2(1 - \frac{t}{T_d})^3 + 3(1 - \frac{t}{T_d})^2 \Bigg), \tag{22}$$

and

$$e_{r,k}(t) = (e_{1,k}(0) + e_{2,k}(0)t) \times \Bigg(6(1 - \frac{t}{T_d})^5 - 15(1 - \frac{t}{T_d})^4 + 10(1 - \frac{t}{T_d})^3 \Bigg), \tag{23}$$

respectively.

In constructing transition trajectory (21), the initial state error $e_{i,k}(0)$ can be set arbitrarily, meaning that the desired error trajectory (8) can be directly applied for systems in the form of (1) with initial state errors. Moreover, the desired error trajectory (8) does not rely on the reference trajectory, and thus it is suitable for the controller design to cope with the iteration-varying trajectory tracking problem. Compared with the previous work in [18], [19], [20], and [21], all the initial values of state errors are considered in constructing transition trajectory, and thus the proposed desired error trajectory is suitable to handle the state tracking issue with arbitrary initial state errors.

Remark 1: It should be noted that the conditions (9) and (10) are only restrictions on the construction of $e^*_{i,k}$, while the initial tracking error, i.e., $e_{i,k}(0)$, is allowed to be set arbitrarily. Consequently, by constructing $e^*_{i,k}$, the constraint on the initial states in conventional ILC can be relaxed in this paper. Moreover, the condition (10) that $e^*_{i,k}(T_d) = 0$ and $\dot{e}^*_{i,k}(T_d) = 0$ can ensure that $e^*_{i,k}(t)$ at the access point T_d becomes smooth and differentiable.

Remark 2: From (15), it follows that the continuous function $\xi(t)$ is constructed in the polynomial form. In fact, there are also some other selections of $\xi(t)$, such as the trigonometric function form, integral form, hyperbolic cosine function form and so on. Compared with those expression forms, the employed polynomial form is more intuitive to be constructed.

Different from the error-tracking approach, the initial rectifying methods in the literatures [14] and [15] can also relax the identical initial condition by constructing rectified reference trajectories. As shown in [14], a rectified reference trajectory is formed by the transition trajectory $r^*_k(t)$, which is written as $r^*_k(t) = A_0t^3 + A_1t^2 + A_2t + A_3$ with four coefficients being dependent on the values $x_{1,k}(0)$, $\dot{x}_{1,k}(0)$, $r_k(T_d)$ and $\dot{r}_k(T_d)$. It means that when operating different tracking tasks in each iteration, the reference signal r_k will be iteration-varying for different k, and the coefficients have to be redesigned in each iteration, which will increase the amount of calculation.

Compared with the initial rectifying methods in [14] and [15], the error attenuation requirement in error tracking approach is more intuitive and clear. In this paper, a simple smooth and continuous error reference trajectory is presented with fewer factors (only two initial factors $e_{i,k}(0)$ and $\dot{e}_{i,k}(0)$) required in the trajectory construction. Due to the independence of the original reference signal r_k, the proposed error trajectory is suitable for coping with the iteration-varying trajectory tracking problem. It means that when operating different tracking tasks in each iteration, there is no need to redesign the error reference trajectory $e^*_{i,k}$.

The control objective is to devise an adaptive fuzzy iterative learning controller for the constrained system (1) with arbitrary initial state errors $e_{i,k}(0)$ and unknown control gain $g(\boldsymbol{x_k})$, such that the state tracking errors $e_{i,k}(t)$ is able to track the desired error trajectory $e^*_{i,k}(t)$ as the iteration increases over the interval $[0, T]$, respectively. It means that the system state vector $\boldsymbol{x_k}$ can follow the iteration-varying reference trajectory $\boldsymbol{r_k} = [x_{d,k}, \dot{x}_{d,k}, \cdots, x^{(n-1)}_{d,k}]^T$ over the interval $[T_d, T]$. Moreover, the tracking error is required to be constrained within the preassigned boundary over the interval $[0, T]$.

IV. Controller Design

Define $z_{i,k}$ and $z_{n,k}$ as

$$z_{i,k} = e_{i,k} - e^*_{i,k}, z_{n,k} = e_{n,k} - e^*_{n,k}. \tag{24}$$

where $i = 1, \cdots, n-1$.

From (4) and (24), it is obtained that

$$\begin{aligned} \dot{z}_{i,k} &= z_{i+1,k}, \\ \dot{z}_{n,k} &= f_{n,k} + h_{n,k}u_k(t) + g_{n,k}o(t) - x^{(n)}_{d,k} - \dot{e}^*_{n,k}, \end{aligned} \tag{25}$$

where $h_{n,k} = g_{n,k}\iota(t)$, and according to the positive function $g_{n,k}$ and the constrained control input (2), one has $h_{n,k} > 0$.

Define the error variable s_k as

$$\begin{aligned} s_k &= [\mathbf{\Lambda}^T, 1]\boldsymbol{z_k} \\ &= c_1 z_{1,k} + c_2 z_{2,k} + \cdots + c_{n-1} z_{n-1,k} + z_{n,k}, \end{aligned} \tag{26}$$

where $\boldsymbol{z_k} = [z_{1,k}, \cdots, z_{n,k}]^T$, $\mathbf{\Lambda} = [c_1, \cdots, c_{n-1}]^T$, and c_i is selected to make the polynomial $P(X) = X^{n-1} + c_{n-1}X^{n-2} + \cdots + c_1$ Hurwitz.

Differentiating (26) yields

$$\begin{aligned} \dot{s}_k &= c_1 z_{2,k} + c_2 z_{3,k} + \cdots + c_{n-1} z_{n,k} + \dot{z}_{n,k} \\ &= h_{n,k}\left(u_k(t) + \bar{o}(t) + \frac{1}{h_{n,k}}\left(f_{n,k} + \sigma_k - \dot{e}^*_{n,k} - x^{(n)}_{d,k}\right)\right), \end{aligned} \tag{27}$$

where $\sigma_k = c_1 z_{2,k} + c_2 z_{3,k} + \cdots + c_{n-1} z_{n,k}$. $\bar{o}(t) = o(t)\iota(t)^{-1}$ and $|\bar{o}(t)| < O_\iota$, with O_ι being an unknown positive constant.

In order to address the asymmetric output constraints, the AIFBLF is constructed as

$$E_{1,k}(t) = \int_0^t \frac{1}{h_{n,k}}\frac{d}{dt}\left(\frac{1}{2}\frac{s_k^2}{(\underline{k}_c + z_{1,k})^2(\bar{k}_c - z_{1,k})^2}\right)d\tau, \tag{28}$$

where $\bar{k}_c, \underline{k}_c > 0$ are the constraints of $z_{1,k}$, i.e., $-\underline{k}_c < z_{1,k} < \bar{k}_c$.

The time derivative of (28) is

$$\dot{E}_{1,k}(t) = \frac{1}{h_{n,k}}\left(\rho_k s_k \dot{s}_k - \frac{s_k^2 z_{2,k}(\bar{k}_c - \underline{k}_c - 2z_{1,k})}{(\bar{k}_c - z_{1,k})^3(\underline{k}_c + z_{1,k})^3}\right), \tag{29}$$

where $\rho_k = \frac{1}{(\bar{k}_c - z_{1,k})^2(\underline{k}_c + z_{1,k})^2} > 0$.

Substituting (27) into (29) leads to

$$\begin{aligned} \dot{E}_{1,k}(t) &= \rho_k s_k\left(u_k(t) + \frac{1}{h_{n,k}}\left(\sigma_k + f_{n,k} - x^{(n)}_{d,k} - \dot{e}^*_{n,k}\right)\right) \\ &\quad + \rho_k s_k \bar{o}(t) - \frac{s_k^2 z_{2,k}(\bar{k}_c - \underline{k}_c - 2z_{1,k})}{h_{n,k}(\bar{k}_c - z_{1,k})^3(\underline{k}_c + z_{1,k})^3} \\ &= \rho_k s_k\left(\bar{h}_{n,k} + u_k(t) + \bar{o}(t)\right), \end{aligned} \tag{30}$$

where $\bar{h}_{n,k} = \frac{1}{h_{n,k}}(\sigma_k - \frac{s_k z_{2,k}(\bar{k}_c - \underline{k}_c - 2z_{1,k})}{(\bar{k}_c - z_{1,k})(\underline{k}_c + z_{1,k})} + f_{n,k} - x^{(n)}_{d,k} - \dot{e}^*_{n,k})$.

The unknown continuous function $\bar{h}_{n,k}$ can be represented by a fuzzy logic system in the form of

$$\bar{h}_{n,k} = W_1^{*T}\Psi(\bar{\boldsymbol{X}}_{1,k}) + \varepsilon_{1,k}, \tag{31}$$

where $W_1^* \in R^{N\times 1}$ is the ideal weight vector, where $N = 3n + 2$. $\Psi(\bar{\boldsymbol{X}}_{1,k})$ is the active function with $\bar{\boldsymbol{X}}_{1,k} = [\boldsymbol{x}_k, \boldsymbol{r}_k, x^{(n)}_{d,k}, e^*_{1,k}, \cdots, e^*_{n,k}, \dot{e}^*_{n,k}]^T$. For the noting convenience, $\Psi_{1,k} = \Psi(\bar{\boldsymbol{X}}_{1,k})$. $\varepsilon_{1,k}$ is the approximated error with $|\varepsilon_{1,k}| \le \varepsilon_{1N}$, and $\varepsilon_{1N} > 0$ is an unknown constant.

Substituting (31) into (30) yields

$$\begin{aligned} \dot{E}_{1,k}(t) &= \rho_k s_k\left(u_k + W_1^{*T}\Psi_{1,k} + \varepsilon_{1,k} + \bar{o}(t)\right) \\ &\le \rho_k s_k\left(u_k + W_1^{*T}\Psi_{1,k}\right) + |\rho_k s_k|(\varepsilon_{1N} + O_\iota) \\ &= \rho_k s_k\left(u_k + W_1^{*T}\Psi_{1,k}\right) + \delta_m|\rho_k s_k|, \end{aligned} \tag{32}$$

where $\delta_m = \varepsilon_{1N} + O_\iota$.

Define $E_k(t)$ as

$$E_k(t) = E_{1,k}(t) + \frac{1-\gamma_1}{2\beta_1}\tilde{W}^T_{1,k}\tilde{W}_{1,k} + \frac{1-\gamma_2}{2\beta_2}\tilde{\delta}^2_{1,k}, \tag{33}$$

where $\tilde{W}_{1,k} = W_1^* - \hat{W}_{1,k}$, $\tilde{\delta}_{1,k} = \delta_m - \hat{\delta}_{1,k}$. $\hat{W}_{1,k}$ and $\hat{\delta}_{1,k}$ are estimates of W_1^* and δ_m, respectively.

Differentiating $E_k(t)$, one has

$$\begin{aligned} \dot{E}_k(t) &\le \rho_k s_k\left(u_k + W_1^{*T}\Psi_{1,k}\right) + \delta_m|\rho_k s_k| \\ &\quad + \frac{1-\gamma_1}{\beta_1}\tilde{W}^T_{1,k}\dot{\tilde{W}}_{1,k} + \frac{1-\gamma_2}{\beta_2}\tilde{\delta}_{1,k}\dot{\tilde{\delta}}_{1,k}, \end{aligned} \tag{34}$$

The adaptive fuzzy iterative learning controller is developed as

$$u_k = -\lambda_1\rho_k^{-1}s_k - \hat{\delta}_{1,k}\mathrm{sgn}(\rho_k s_k) - \hat{W}^T_{1,k}\Psi_{1,k}. \tag{35}$$

The combined adaptive learning laws of $\hat{W}_{1,k}$, $\hat{\delta}_{1,k}$ are developed as

$$(1-\gamma_1)\dot{\hat{W}}_{1,k} = -\gamma_1\hat{W}_{1,k} + \gamma_1\hat{W}_{1,k-1} + \beta_1\rho_k s_k\Psi_{1,k}, \tag{36}$$

and

$$(1-\gamma_2)\dot{\hat{\delta}}_{1,k} = -\gamma_2\hat{\delta}_{1,k} + \gamma_2\hat{\delta}_{1,k-1} + \beta_2|\rho_k s_k|, \tag{37}$$

where $\hat{W}_{1,k}(0) = \hat{W}_{1,k-1}(T)$, $\hat{\delta}_{1,k}(0) = \hat{\delta}_{1,k-1}(T)$, $\hat{W}_{1,-1}(t) = 0$, and $\hat{\delta}_{1,-1}(t) = 0$.

Remark 3: To avoid the chattering phenomenon arising from the sign function in (35), one can replace it by the boundary layer technique or the hyperbolic tangent function.

Remark 4: Different from adaptive control methods, the proposed adaptive iterative learning control method can not only effectively handle the uncertainty of the system, but also gradually optimize tracking performance with the increase of iteration numbers, achieving complete tracking of the reference trajectory in a finite time. In addition, the proposed AIFBLF (28) is constructed to keep the system tracking error within a predetermined boundary in each iteration. Compared with the asymmetric BLFs [52], [54], the proposed AIFBLF does not require the discontinuous function or increasing the error variable to high power. Compared with [52], [54], and [56], the unknown control gain function $h_{n,k}$ is handled by designing the AIFBLF in this paper, such that the control design in this paper does not require estimating the unknown control gain function or using the bounds of the gain function differentiation, and thus the computational burden is decreased.

V. Convergence Analysis

Theorem 1: For a constrained system (1) with arbitrary initial state errors and unknown control gain, by constructing the desired error trajectory (8), the adaptive fuzzy iterative learning controller (35) and the combined adaptive learning laws (36), (37), the following properties are guaranteed:

i) $\lim_{k\to\infty} s_k^2(t) = 0, \forall t \in [0, T]$;

ii) the system output $x_{1,k}$ can be constrained within the asymmetric constraints over the interval $t \in [0, T]$, and all system variables are bounded.

Proof: Define a Lyapunov-like function $L_k(t)$ as

$$L_k(t) = E_k(t) + \frac{\gamma_1}{2\beta_1}\int_0^t\left(\tilde{W}^T_{1,k}\tilde{W}_{1,k}\right)d\tau + \frac{\gamma_2}{2\beta_2}\int_0^t\tilde{\delta}^2_{1,k}d\tau. \tag{38}$$

The proof process includes four steps. First, the boundedness of $L_0(t)$ on $[0, T]$ is proved. Second, the boundedness of all system variables is analyzed. Third, the convergence of the s_k is proved. Fourth, the satisfaction of the constraint requirements is provided.

1) Step I: The boundedness of $L_0(t)$.

Differentiating $E_k(t)$, one has

$$\dot{E}_k(t) \leq \rho_k s_k\big(u_k + W_1^{*T}\Psi_{1,k}\big) + \delta_m|\rho_k s_k| + \frac{1-\gamma_1}{\beta_1}\tilde{W}_{1,k}^T\dot{\tilde{W}}_{1,k} + \frac{1-\gamma_2}{\beta_2}\tilde{\delta}_{1,k}\dot{\tilde{\delta}}_{1,k}. \tag{39}$$

Substituting (35) into (39) obtains

$$\dot{E}_k(t) \leq -\lambda_1 s_k^2 + \rho_k s_k\tilde{W}_{1,k}^T\Psi_{1,k} + \tilde{\delta}_{1,k}|\rho_k s_k| - \frac{1-\gamma_1}{\beta_1}\tilde{W}_{1,k}^T\dot{\hat{W}}_{1,k} - \frac{1-\gamma_2}{\beta_2}\tilde{\delta}_{1,k}\dot{\hat{\delta}}_{1,k}. \tag{40}$$

Substituting (36) and (37) into (40) yields

$$\begin{aligned}\dot{E}_k(t) \leq& -\frac{1}{\beta_1}\tilde{W}_{1,k}^T\big(-\gamma_1\hat{W}_{1,k} + \gamma_1\hat{W}_{1,k-1} + \beta_1\rho_k s_k\Psi_{1,k}\big)\\ &-\frac{1}{\beta_2}\tilde{\delta}_{1,k}\big(-\gamma_2\hat{\delta}_{1,k} + \gamma_2\hat{\delta}_{1,k-1} + \beta_2|\rho_k s_k|\big)\\ =& -\lambda_1 s_k^2 - \frac{\gamma_1}{\beta_1}\tilde{W}_{1,k}^T\big(-\hat{W}_{1,k} + \hat{W}_{1,k-1}\big)\\ &-\frac{\gamma_2}{\beta_2}\tilde{\delta}_{1,k}\big(-\hat{\delta}_{1,k} + \hat{\delta}_{1,k-1}\big).\end{aligned} \tag{41}$$

Differentiating $L_k(t)$ yields

$$\dot{L}_k(t) = \dot{E}_k(t) + \frac{\gamma_1}{2\beta_1}\tilde{W}_{1,k}^T\tilde{W}_{1,k} + \frac{\gamma_2}{2\beta_2}\tilde{\delta}_{1,k}^2. \tag{42}$$

Substituting (41) into (42) yields

$$\begin{aligned}\dot{L}_k(t) \leq& -\lambda_1 s_k^2 - \frac{\gamma_1}{2\beta_1}(\tilde{W}_{1,k-1} - \tilde{W}_{1,k})^T(\tilde{W}_{1,k-1} - \tilde{W}_{1,k})\\ &-\frac{\gamma_2}{2\beta_2}(\tilde{\delta}_{1,k-1} - \tilde{\delta}_{1,k})^2 + \frac{\gamma_2}{2\beta_2}(\tilde{\delta}_{1,k-1}^2 - \tilde{\delta}_{1,k}^2)\\ &+\frac{\gamma_1}{2\beta_1}(\tilde{W}_{1,k-1}^T\tilde{W}_{1,k-1} - \tilde{W}_{1,k}^T\tilde{W}_{1,k})\\ &+\frac{\gamma_1}{2\beta_1}\tilde{W}_{1,k}^T\tilde{W}_{1,k} + \frac{\gamma_2}{2\beta_2}\tilde{\delta}_{1,k}^2\\ \leq& -\lambda_1 s_k^2 + \frac{\gamma_1}{2\beta_1}\tilde{W}_{1,k-1}^T\tilde{W}_{1,k-1} + \frac{\gamma_2}{2\beta_2}\tilde{\delta}_{1,k-1}^2.\end{aligned} \tag{43}$$

When $k = 0$, $\hat{W}_{1,-1} = 0$, $\hat{\delta}_{1,-1} = 0$, one has $\tilde{W}_{1,-1} = W_1^*$ and $\tilde{\delta}_{1,-1} = \delta_m$ which are bounded values. It means that $\dot{L}_0(t)$ is rewritten as

$$\begin{aligned}\dot{L}_0(t) \leq& -\lambda_1 s_0^2 + \frac{\gamma_1}{2\beta_1}\tilde{W}_{1,-1}^T\tilde{W}_{1,-1} + \frac{\gamma_2}{2\beta_2}\tilde{\delta}_{1,-1}^2\\ \leq& \frac{\gamma_1}{2\beta_1}W_1^{*T}W_1^* + \frac{\gamma_2}{2\beta_2}\delta_m^2.\end{aligned} \tag{44}$$

Integrating both side of (44) leads to

$$\begin{aligned}L_0(t) \leq& L_0(0) + \int_0^t\left(\frac{\gamma_1}{2\beta_1}W_1^{*T}W_1^* + \frac{\gamma_2}{2\beta_2}\delta_m^2\right)d\tau\\ \leq& E_0(0) + \int_0^t\left(\frac{\gamma_1}{2\beta_1}W_1^{*T}W_1^* + \frac{\gamma_2}{2\beta_2}\delta_m^2\right)d\tau.\end{aligned} \tag{45}$$

From the constructed error trajectory (8), the condition (9) is satisfied, thus $s_k(0) = 0$ can be obtained. According to $s_0(0) = 0$ and the selection of initial value $\hat{W}_{1,-1} = 0$, it can be obtained the boundedness of $E_0(0)$. From the boundedness of $\int_0^t\left(\frac{\gamma_1}{2\beta_1}W_1^{*T}W_1^* + \frac{\gamma_2}{2\beta_2}\delta_m^2\right)d\tau$ on $[0, T]$, $L_0(t)$ is bounded on $[0, T]$, i.e.,

$$\begin{aligned}L_0(t) \leq& E_0(0) + \int_0^T\left(\frac{\gamma_1}{2\beta_1}W_1^{*T}W_1^* + \frac{\gamma_2}{2\beta_2}\delta_m^2\right)d\tau\\ <& \infty.\end{aligned} \tag{46}$$

2) Step II: The boundedness of all system variables.

The difference of $L_k(t)$ is written as

$$\begin{aligned}\Delta L_k(t) =& E_k(0) + \int_0^t\dot{E}_k(\tau)d\tau - E_{k-1}(t)\\ &+\frac{\gamma_1}{2\beta_1}\int_0^t\big(\tilde{W}_{1,k}^T\tilde{W}_{1,k} - \tilde{W}_{1,k-1}^T\tilde{W}_{1,k-1}\big)d\tau\\ &+\frac{\gamma_2}{2\beta_2}\int_0^t\big(\tilde{\delta}_{1,k}^2 - \tilde{\delta}_{1,k-1}^2\big)d\tau\\ \leq& E_k(0) - E_{k-1}(t)\\ &-\frac{\gamma_1}{\beta_1}\int_0^t\left(\tilde{W}_{1,k}^T(\hat{W}_{1,k} - \hat{W}_{1,k-1})\right)d\tau\\ &-\frac{\gamma_2}{\beta_2}\int_0^t\left(\tilde{\delta}_{1,k}(\hat{\delta}_{1,k} - \hat{\delta}_{1,k-1})\right)d\tau + \int_0^t\dot{E}_k(\tau)d\tau.\end{aligned} \tag{47}$$

Substituting (41) into (47) leads to

$$\begin{aligned}\Delta L_k(t) \leq& E_k(0) - E_{k-1}(t) - \lambda_1\int_0^t s_k^2 d\tau\\ =& E_{1,k}(0) - E_{1,k-1}(T) + \frac{1-\gamma_1}{2\beta_1}\tilde{W}_{1,k}^T(0)\tilde{W}_{1,k}(0)\\ &-\frac{1-\gamma_1}{2\beta_1}\tilde{W}_{1,k-1}^T(T)\tilde{W}_{1,k-1}(T) - \lambda_1\int_0^T s_k^2 d\tau\\ &+\frac{1-\gamma_2}{2\beta_2}\tilde{\delta}_{1,k}^2(0) - \frac{1-\gamma_2}{2\beta_2}\tilde{\delta}_{1,k-1}^2(T)\\ \leq& -\lambda_1\int_0^T s_k^2 d\tau.\end{aligned} \tag{48}$$

$\Delta L_k(T)$ is negative definite which can be get from (48), and $L_0(T)$ is bounded from (46). Thus, $L_k(T) = L_0(T) + \sum_{j=1}^{k}\Delta L_j(T)$ is bounded. Therefore, for $\forall t \in [0, T]$, there exist finite and positive constants $M_1, M_2, M_3, M_4 > 0$, such that

$$\begin{aligned}&\frac{\gamma_1}{2\beta_1}\int_0^t\big(\tilde{W}_{1,k}^T\tilde{W}_{1,k}\big)d\tau + \frac{\gamma_2}{2\beta_2}\int_0^t\tilde{\delta}_{1,k}^2 d\tau\\ &\leq \frac{\gamma_1}{2\beta_1}\int_0^T\big(\tilde{W}_{1,k}^T\tilde{W}_{1,k}\big)d\tau + \frac{\gamma_2}{2\beta_2}\int_0^T\tilde{\delta}_{1,k}^2 d\tau\\ &\leq M_1 < \infty.\end{aligned} \tag{49}$$

$$\begin{aligned}&\frac{1-\gamma_1}{2\beta_1}\tilde{W}_{1,k}(T)^T\tilde{W}_{1,k}(T) + \frac{1-\gamma_2}{2\beta_2}\tilde{\delta}_{1,k}^2(T)\\ &\leq M_2 < \infty.\end{aligned} \tag{50}$$

Substituting (49) into (38) yields

$$\begin{aligned}L_k(t) \leq& \int_0^t\frac{1}{h_{n,k}}\frac{d}{dt}\left(\frac{1}{2}\frac{s_k^2}{(\underline{k}_c + z_{1,k})^2(\bar{k}_c - z_{1,k})^2}\right)d\tau\\ &+\frac{1-\gamma_1}{2\beta_1}\tilde{W}_{1,k}^T\tilde{W}_{1,k} + \frac{1-\gamma_2}{2\beta_2}\tilde{\delta}_{1,k}^2 + M_1.\end{aligned} \tag{51}$$

From (48), it can be obtained as

$$\begin{aligned}\Delta L_k(t) &\le E_k(0) - E_{k-1}(t) - \lambda_1 \int_0^t s_k^2 d\tau \\ &\le E_k(0) - E_{k-1}(t).\end{aligned} \tag{52}$$

Substituting (50) into (52) yields

$$\begin{aligned}&\Delta L_k(t) \\ &= \frac{1-\gamma_1}{2\beta_1}\tilde{W}_{1,k-1}(T)^T\tilde{W}_{1,k-1}(T) + \frac{1-\gamma_2}{2\beta_2}\tilde{\delta}^2_{1,k-1}(T) \\ &\quad - \frac{1-\gamma_1}{2\beta_1}\tilde{W}_{1,k-1}(t)^T\tilde{W}_{1,k-1}(t) - \frac{1-\gamma_2}{2\beta_2}\tilde{\delta}^2_{1,k-1}(t) \\ &\quad - \int_0^t \frac{1}{h_{n,k-1}}\frac{d}{dt}\left(\frac{1}{2}\frac{s_{k-1}^2}{(\underline{k}_c + z_{1,k-1})^2(\overline{k}_c - z_{1,k-1})^2}\right)d\tau \\ &\le M_2 - \frac{1-\gamma_1}{2\beta_1}\tilde{W}_{1,k-1}(t)^T\tilde{W}_{1,k-1}(t) - \frac{1-\gamma_2}{2\beta_2}\tilde{\delta}^2_{1,k-1}(t) \\ &\quad - \int_0^t \frac{1}{h_{n,k-1}}\frac{d}{dt}\left(\frac{1}{2}\frac{s_{k-1}^2}{(\underline{k}_c + z_{1,k-1})^2(\overline{k}_c - z_{1,k-1})^2}\right)d\tau.\end{aligned} \tag{53}$$

When $k = k+1$, $\Delta L_{k+1}(t)$ can be written as

$$\begin{aligned}\Delta L_{k+1}(t) &\le M_2 - \frac{1-\gamma_1}{2\beta_1}\tilde{W}_{1,k}^T\tilde{W}_{1,k} - \frac{1-\gamma_2}{2\beta_2}\tilde{\delta}^2_{1,k} \\ &\quad - \int_0^t \frac{1}{h_{n,k}}\frac{d}{dt}\left(\frac{1}{2}\frac{s_k^2}{(\underline{k}_c + z_{1,k})^2(\overline{k}_c - z_{1,k})^2}\right)d\tau.\end{aligned} \tag{54}$$

By combining (51) and (54), $L_{k+1}(t)$ is rewritten as

$$\begin{aligned}L_{k+1}(t) &= L_k(t) + \Delta L_{k+1}(t) \\ &\le M_1 + M_2 < \infty.\end{aligned} \tag{55}$$

From (46) and (55), one has $L_k(t)$ is bounded. According to the combined adaptive laws (36), (37) and the definition of $L_k(t)$ in (38), $\hat{W}_{1,k}$ and $\hat{\delta}_{1,k}$ are uniformly bounded. Combining (3), (24), (26) and (35), uniform boundedness of the $\boldsymbol{z_k}$, $\boldsymbol{x_k}$, s_k and u_k can be obtained. From (8) and (27), and using the uniform boundedness of $e^*_{i,k}$, $\dot{e}^*_{i,k}$, u_k and $\boldsymbol{z_k}$, one has that $\dot{s}_k$ is uniformly bounded. In summary, all system variables are uniformly bounded.

3) Step III: The tracking convergence of s_k. $\lim_{k\to\infty} L_k(T)$ can be written as

$$\begin{aligned}\lim_{k\to\infty} L_k(T) &\le L_0(T) + \lim_{k\to\infty}\sum_{j=1}^{k}\left[-\lambda_1\int_0^T s_j^2 d\tau\right] \\ &= L_0(T) - \lim_{k\to\infty}\lambda_1\sum_{j=1}^{k}\int_0^T s_j^2 d\tau.\end{aligned} \tag{56}$$

From the boundedness of $L_0(t)$, the positive define of $L_k(t)$, and (56), it can be obtained that

$$\lim_{k\to\infty}\lambda_1\sum_{j=1}^{k}\int_0^T s_j^2 d\tau = 0. \tag{57}$$

According to the Lemma 1 and (57), the convergence of s_k can be obtained, i.e.,

$$\lim_{k\to\infty} s_k^2(t) = 0, \forall t \in [0, T]. \tag{58}$$

4) Step IV: Satisfaction of the constraint requirements

According to the above analysis, one has that s_k and L_k are bounded, and thus $-\underline{k}_c < z_{1,k} < \overline{k}_c$ is guaranteed. From (8), $e^*_{i,k}$ is bounded. From the definition of $z_{1,k}$, one has $e_{1,k} = z_{1,k} + e^*_{1,k}$, which implies that $e_{1,k}$ is bounded. Since $x_{1,k} = z_{1,k} + x_{d,k} + e^*_{1,k}$, let $-\underline{k}_b = -\underline{k}_c + x_{d,k} + e^*_{1,k}$, $\overline{k}_b = \overline{k}_c + x_{d,k} + e^*_{1,k}$, one has $-\underline{k}_b < x_{1,k} < \overline{k}_b$, and thus $x_{1,k}$ is bounded.

Remark 5: The selection of parameters in (35)-(37) is crucial for error convergence performance. The increase of λ_1, β_1 and β_2 can accelerate the convergence of error. However, excessive λ_1, β_1 and β_2 may lead to high-gain control issues. Therefore, careful consideration should be given to the balance between error convergence and controller gain when selecting parameters λ_1, β_1 and β_2. The parameters γ_1 and γ_2 should be chosen over the range [0, 1].

Remark 6: The combined adaptive laws (36) and (37) are developed to restrain the ceaseless positive accumulation issue by using the leakage terms $-\gamma_1\hat{W}_{1,k}$ and $-\gamma_2\hat{\delta}_{1,k}$, in the case that γ_1 and γ_2 are chosen over the range (0, 1). When γ_1 and γ_2 are selected as the boundary values, i.e., $\gamma_1 = \gamma_2 = 1$, $\gamma_1 = \gamma_2 = 0$, the combined adaptive learning laws are turned into pure iterative learning laws [56] and adaptive laws [58], respectively.

VI. Numerical Simulation and Experiments

A. Simulation: A Constrained One-Link Robotic Manipulator

A one-link robotic manipulator is formulated as [7]

$$\begin{cases}\dot{x}_{1,k} = x_{2,k} \\ \dot{x}_{2,k} = \dfrac{mgl}{J}\sin(x_{1,k}) + \dfrac{1}{J}\psi(u_k),\end{cases} \tag{59}$$

where $x_{1,k}$ is the joint angle; $x_{2,k}$ is the angular velocity; l and m are the length and mass of the manipulator, respectively; g is the gravity. The constrained control input $\psi(u_k)$ is expressed as

$$\psi(u_k) = \begin{cases}\psi_{\max}, & u_k \ge s_p \\ \psi_r(u_k), & d_p \le u_k < s_p \\ 0, & d_n \le u_k < d_p \\ \psi_l(u_k), & s_n \le u_k < d_n \\ \psi_{\min}, & u_k < s_n,\end{cases} \tag{60}$$

with $\psi_r(u_k) = (s_p - 2 + 2\sin(\frac{5\pi}{2s_p}u_k))\frac{(u_k - d_p)}{s_p - d_p}$, $\psi_l(u_k) = (s_n + 2 - 2\sin(\frac{5\pi}{2s_n}u_k))\frac{(u_k - d_n)}{s_n - d_n}$, and $s_p = 15$, $d_p = 1.5$, $s_n = -15$, $d_n = -1.5$, $\psi_{\max} = 15$ and $\psi_{\min} = -15$.

The system parameters are set as: $m = 2.3$kg, $J = 1.1667\text{kg}\cdot\text{m}^2$, $g = 9.8\text{m}\cdot\text{s}^{-2}$, $l = 0.9$m, and the iteration number is set as $K = 10$. $J_k \triangleq \max_{t\in[0,T]}|z_{1,k}(t)|$. $x_{d,k} = (0.3 + 0.01\frac{k}{K})\sin((1 + 0.01\frac{k}{K})t) + 0.2\cos(t)$, where k is the current iteration. $\boldsymbol{x_k}(0) = [0.25 + 0.02\text{rand}(1), 0.33 + 0.02\text{rand}(1)]^T$. $T = 12$s, and $T_d = 0.4$s.

To verify the efficacy of the proposed AFILC method, two other different AILC methods in [14] and [19] and an adaptive fuzzy control method with output constraint in [22] are given for performance comparison.

1) M1: The Proposed AFILC Method: For the one-link robotic manipulator (59), the desired error trajectory and the transition trajectory are given as (8) and (23) in the section III, respectively. The adaptive fuzzy iterative learning controller and update laws are given as (35)-(37), respectively. The parameters are set as $c_1 = 1$, $\lambda_1 = 6$, $\gamma_1 = 0.9$, $\beta_1 = 2.5$, $\gamma_2 = 0.6$ and $\beta_2 = 12$. The active function in the FLSs is given as $\psi(\bar{X}_{1,k}) = e^{-(\bar{X}_{1,k}-L_j)^2/10}$, and $L = [6, 5, 4, 3, 2, 1, 0, -1, -2, -3, -4, -5, -6]^T$. The asymmetric constraint of $z_{1,k}$ is chosen as $\bar{k}_c = 0.2$, $\underline{k}_c = 0.15$.

2) M2: The Neural AILC Method in [19]: In the M2 method, $e^*_{1,k}$ is given as

$$e^*_{1,k}(t) = \begin{cases} e_{r,k}(t), & t \in [0, T_d] \\ 0, & t \in (T_d, T], \end{cases} \tag{61}$$

where

$$e_{r,k}(t) = e_{1,k}(0) \times \left(6(1-\frac{t}{T_d})^5 - 15(1-\frac{t}{T_d})^4 + 10(1-\frac{t}{T_d})^3\right), \tag{62}$$

and $e^*_{2,k}(t) = \dot{e}^*_{1,k}(t)$.

Define $\upsilon_{1,k}$, $s_{\varepsilon,k}$, ι_k and ς_k as

$$\upsilon_{1,k} = c_1 z_{2,k} - \ddot{x}_{d,k} - \dot{e}^*_{2,k}, \tag{63}$$

$$s_{\varepsilon,k} = |s_k| - \varepsilon, \tag{64}$$

$$\iota_k = \iota(s_k) = \begin{cases} 1, & \text{if} \quad |s_k| > \varepsilon \\ 0, & \text{if} \quad |s_k| \le \varepsilon, \end{cases} \tag{65}$$

$$\varsigma_k = \varsigma(s_k) = \begin{cases} \text{sgn}(s_k), & \text{if} \quad |s_k| > \varepsilon \\ 0, & \text{if} \quad |s_k| \le \varepsilon, \end{cases} \tag{66}$$

where $\varepsilon = 0.001$.

The controller and update laws are designed as

$$u_k = -\lambda_1 s_{\varepsilon,k}\varsigma_k - \hat{W}^T_{a,k}\Psi_{a,k} - \hat{W}^T_{b,k}\Psi_{b,k}\upsilon_{1,k} - (\hat{\theta}_{a,k} + \hat{\theta}_{b,k}|\upsilon_{1,k}|)\varsigma_k, \tag{67}$$

and

$$\begin{aligned} &\hat{W}_{a,k} = \text{sat}(W_{a,k}),\ W_{a,k} = \text{sat}(W_{a,k-1}) + \gamma_1 s_{\varepsilon,k}\Psi_{a,k}\varsigma_k, \\ &\hat{W}_{b,k} = \text{sat}(W_{b,k}),\ W_{b,k} = \text{sat}(W_{b,k-1}) + \gamma_2 s_{\varepsilon,k}\Psi_{b,k}\upsilon_{1,k}\varsigma_k, \\ &\hat{\theta}_{a,k} = \text{sat}(\theta_{a,k}),\ \theta_{a,k} = \text{sat}(\theta_{a,k-1}) + \gamma_3 s_{\varepsilon,k}\iota_k, \\ &\hat{\theta}_{b,k} = \text{sat}(\theta_{b,k}),\ \theta_{b,k} = \text{sat}(\theta_{b,k-1}) + \gamma_4 s_{\varepsilon,k}|\upsilon_{1,k}|\iota_k. \end{aligned} \tag{68}$$

The control gain parameters in (67) are the same as those in M1 method. Besides, the parameters in (68) are set as $\gamma_1 = 10$, $\gamma_2 = 10$, $\gamma_3 = 0.02$, $\gamma_4 = 0.02$. The parameters of the active function $\psi(\bar{X}_{1,k}) = a_m/(b_m + e^{(-\bar{X}_{1,k}/c_m)}) + d_m$ in the neural network are set as $a_m = -1.2$, $b_m = 1$, $c_m = 1$, $d_m = -2$.

3) M3: The AILC Method With the Rectifying Action in [14]: The rectified reference trajectory is given as

$$x^*_{1,k}(t) = \begin{cases} x_r(t), & t \in [0, T_d] \\ x_{d,k}(t), & t \in (T_d, T], \end{cases} \tag{69}$$

where $x_r(t) = a_5 t^5 + a_4 t^4 + a_3 t^3 + a_2 t^2 + a_1 t + a_0$, and

$$\begin{aligned} a_0 &= x_{1,k}(0),\ a_1 = \dot{x}_{1,k}(0),\ a_2 = \frac{1}{2}\ddot{x}_{1,k}(0), \\ a_3 &= -\frac{1}{2T_d^3}(20x_{1,k}(0) - 20x_{d,k}(T_d) + 12T_d\dot{x}_{1,k}(0) \\ &\quad + 8T_d\dot{x}_{d,k}(T_d) + 3T_d^2\ddot{x}_{1,k}(0) - T_d^2\ddot{x}_{d,k}(T_d)), \\ a_4 &= \frac{1}{T_d^4}(15x_{1,k}(0) - 15x_{d,k}(T_d) + 8T_d\dot{x}_{1,k}(0) \\ &\quad + 7T_d\dot{x}_{d,k}(T_d) + 1.5T_d^2\ddot{x}_{1,k}(0) - T_d^2\ddot{x}_{d,k}(T_d)), \\ a_5 &= -\frac{1}{2T_d^5}(12x_{1,k}(0) - 12x_{d,k}(T_d) + 6T_d\dot{x}_{1,k}(0) \\ &\quad + 6T_d\dot{x}_{d,k}(T_d) + T_d^2\ddot{x}_{1,k}(0) - T_d^2\ddot{x}_{d,k}(T_d)). \end{aligned} \tag{70}$$

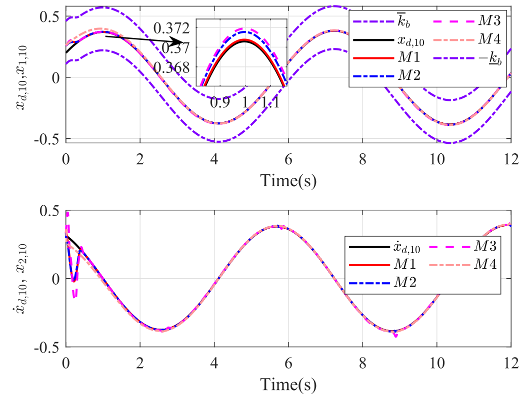

Fig. 2. The tracking performance of the system (59) output $x_{1,k}$ at 10th iteration.

The controller and the update laws are designed as

$$u_k = -\lambda_1 s_k - \hat{W}^T_{1,k}\Psi_{1,k} - \hat{\delta}_{1,k}\text{sgn}(s_k), \tag{71}$$

and

$$(1-\gamma_1)\dot{\hat{W}}_{1,k} = -\gamma_1\hat{W}_{1,k} + \gamma_1\hat{W}_{1,k-1} + \beta_1 s_k\Psi_{1,k}. \tag{72}$$

$$(1-\gamma_2)\dot{\hat{\delta}}_{1,k} = -\gamma_2\hat{\delta}_{1,k} + \gamma_2\hat{\delta}_{1,k-1} + \beta_2|s_k|. \tag{73}$$

The parameters in (71)-(73) are chosen as $c_1 = 1$, $\lambda_1 = 6$, $\gamma_1 = 0.9$, $\beta_1 = 0.2$, $\gamma_2 = 0.6$ and $\beta_2 = 12$. Besides, the active function in the FLSs is given as $\psi(\bar{X}_{1,k}) = e^{-(\bar{X}_{1,k}-L_j)^2/10}$, and $L = [6, 5, 4, 3, 2, 1, 0, -1, -2, -3, -4, -5, -6]^T$.

4) M4: The Adaptive Fuzzy Control Method With Output Constraint in [22]: For fairness in comparison, M4 adopts the same AIFBLF as M1. The errors are defined as $e_1 = x_1 - x_d$, $e_2 = x_2 - \dot{x}_d$, and $s = c_1 e_1 + e_2$. The controller and the update laws are designed as

$$u = -\lambda_1\rho^{-1}s - \hat{\delta}_1\text{sgn}(\rho s) - \hat{W}^T_1\Psi_1. \tag{74}$$

and

$$\dot{\hat{W}}_1 = \beta_1\rho s\Psi_1 - \kappa_1\hat{W}_1. \tag{75}$$

$$\dot{\hat{\delta}}_1 = \beta_2\rho|s| - \kappa_2\hat{\delta}_1. \tag{76}$$

where $\rho = \frac{1}{(\bar{k}_c - e_1)^2(\underline{k}_c + e_1)^2} > 0$, and λ_1, β_i and κ_i, $i = 1, 2$ are positive constants.

The parameters in (74)-(76) are chosen as $c_1 = 1$, $\lambda_1 = 6$, $\kappa_1 = 0.9$, $\beta_1 = 2.5$, $\kappa_2 = 0.6$ and $\beta_2 = 12$. The active function in the FLSs is given as $\psi(\bar{X}_1) = e^{-(\bar{X}_1-L_j)^2/10}$, and $L = [6, 5, 4, 3, 2, 1, 0, -1, -2, -3, -4, -5, -6]^T$. The asymmetric constraint of e_1 is chosen as $\bar{k}_c = 0.2$, $\underline{k}_c = 0.15$.

The simulation results of different control methods for a one-link robotic manipulator after 10th iterations are shown

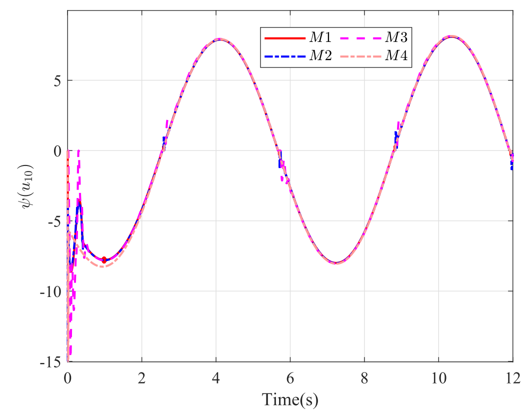

Fig. 3. The constrained control input $\psi(u_k)$ at 10th iteration.

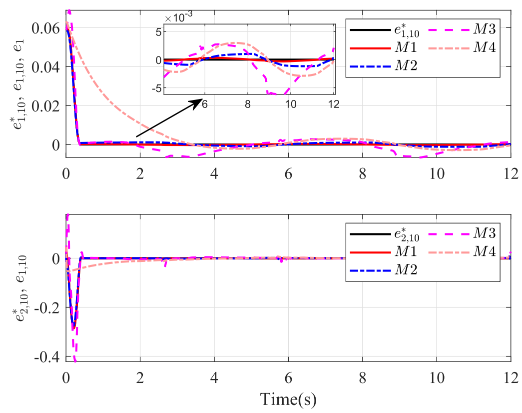

Fig. 4. The tracking performance of the state errors $e_{1,k}$ and $e_{2,k}$ at 10th iteration.

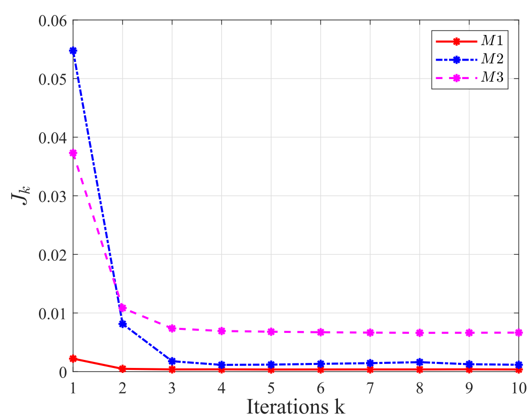

Fig. 5. The performance index J_k of the system (59).

in Figs. 2-5. Fig. 2 indicates that M1-M4 methods could all guarantee that the joint angle converges to the iteration-varying trajectory $x_{d,k}$ with initial state errors. Compared with M2-M4 methods, the proposed M1 method can achieve higher steady-state convergence accuracy for the joint angle $x_{1,k}$. Due to the constructed the AIFBLF, the joint angle $x_{1,k}$ is constrained within the asymmetric constraints over the interval $t \in [0, T]$ after 10th iteration. The control inputs of M1-M3 methods are depicted in Fig. 3, and all of them are constrained within the $\psi_{\max}$ and $\psi_{\min}$. Figs. 4 and 5 show the error tracking performance, and error under the M1 method can be reduced to less than 4×10^{-4}. The tracking performance index in Fig. 5 shows that J_k decreases to a small neighborhood around zero as the number of iterations increases, and the lower performance index of M1 J_k means great control performance.

In summary, from Figs. 2-5, the tracking errors of joint angle and the angle velocity, i.e., $e_{1,10}$ and $e_{2,10}$ can rapidly converge to $e^*_{1,10}$ and $e^*_{2,10}$, and the performance index J_k of M1 has faster convergence under the proposed method.

TABLE I
THE PARAMETERS OF THE PMSM

Name	Parameters(unit)	Value
Moment of Inertia	$J(kg \cdot m^2)$	0.000275
Load Torque	$T_L(N \cdot m)$	$1.5\sin(\theta)$
Flux Linkage	$\varphi_f(Wb)$	0.109
Pole Pairs	n_p	4
Force Coefficient	B	0.0012

B. Experiment: Permanent Magnet Synchronous Motor System(PMSM)

In this section, experiments are illustrated to verify the effectiveness of the proposed approach.

1) Experimental Platform: The overview of the permanent magnet synchronous motor experimental platform is shown in Fig.6, including the PMSM and load, control board, DC power, Emulator, and Computer. A three-phase permanent magnet synchronous motor is applied in the experiment with a rated load, voltage, and power of 1.8N $\cdot$ m, 250VAC, and 570W, respectively. The three-phase inverter used to drive the PMSM is an intelligent power module (IPM) PS21A79. The main control chip on the control board is TMS320F28335 from Texas Instruments, which is connected to a computer with CCS12.0 programming environment. The angular position is measured by an incremental encoder (resolution: 5000pulse/r) and the phase current is measured by the TMS320F28335 ADC module. The 300V DC bus voltage is generated by a DC power supply KPS3005D. The experimental data is sent to the computer by serial communication and processed by the MATLAB.

2) Experimental Results: The PMSM servo systems in the d-q reference coordination is described as

$$\begin{cases} \dot{\theta}_k = \omega_k \\ \dot{\omega}_k = -\dfrac{B}{J}\omega_k + \dfrac{3n_p\varphi_f}{2J}\psi(i_{q,k}) - \dfrac{T_L(\theta_k)}{J} \end{cases} \tag{77}$$

where θ_k is the angular position; ω_k represents the angular speed; J is the inertia of the PMSM; φ_f is the flux linkage; n_p is the number of pole pairs; B is the friction coefficient; $T_L(\theta_k)$ represents the load torque; $\psi(i_{q,k})$ is the constrained q axis stator current, which can be expressed as $\psi(i_{q,k}) = \mathrm{sat}(i_{q,k})$,

$$\mathrm{sat}(i_{q,k}) = \begin{cases} i_{q,\max} & i_{q,k} \geq i_{q,\max} \\ i_{q,k} & i_{q,\min} < i_{q,k} < i_{q,\max} \\ i_{q,\min} & i_{q,k} \leq i_{q,\min}, \end{cases} \tag{78}$$

with $i_{q,\max} = 5$ and $i_{q,\min} = -5$. The parameters of the PMSM is given in the following Table I.

The iteration number is set as $K = 15$, and $x_{d,k} = a_k \sin(t)$rad, where $a_k = 1 + 0.05(1 - \frac{k}{K})$. The initial state is given as $\theta_k(0) = 0.3 + 0.02\mathrm{rand}(1)$rad, $\omega_k(0) = 4$rad/s. $J_k \triangleq \|z_{1,k}(t)\|_2$, $T = 4$s, and $T_d = 0.8$s.

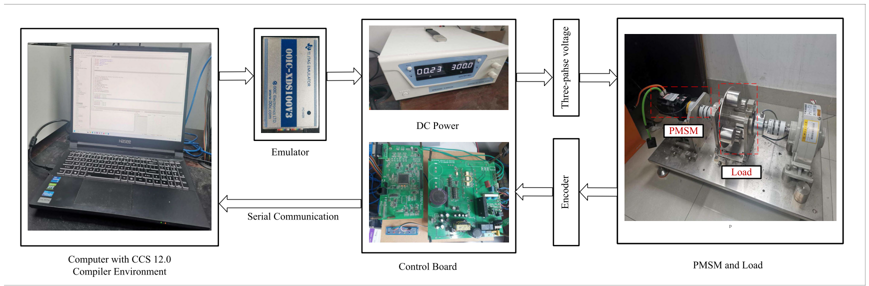

Fig. 6. The overview of the permanent magnet synchronous motor experimental platform.

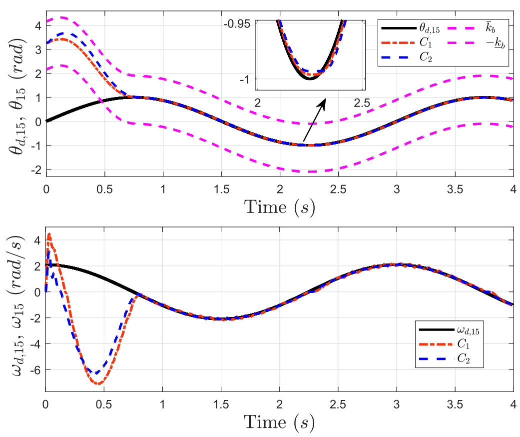

Fig. 7. The tracking performance of the system (77) output θ_k at 15th iteration.

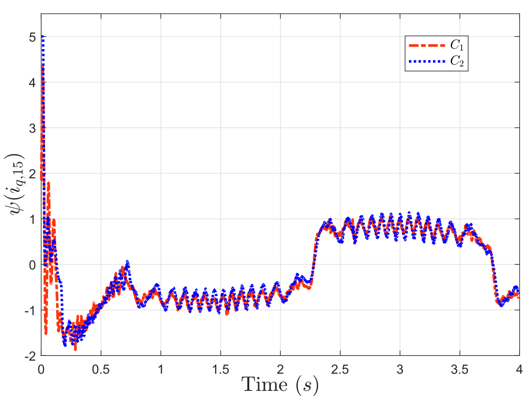

Fig. 8. The constrained control input $\psi(i_{q,k})$ at 15th iteration.

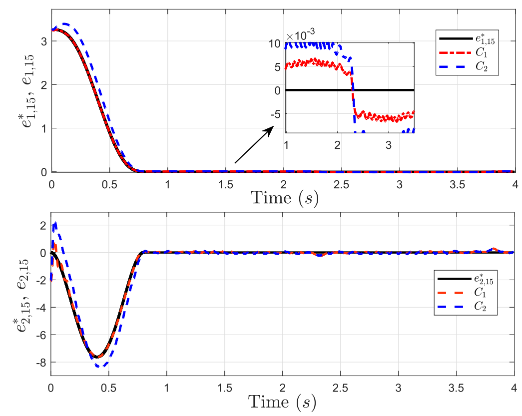

Fig. 9. The tracking performance of $e_{1,k}$ and $e_{2,k}$ at 15th iteration.

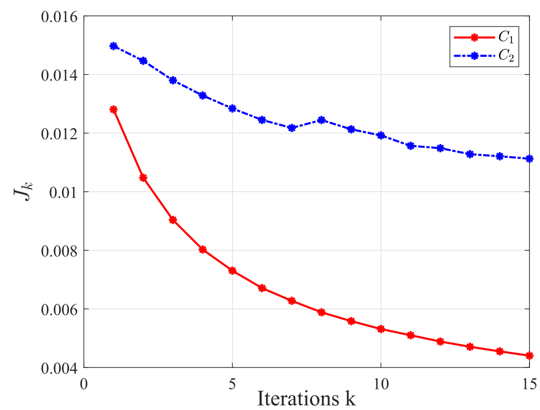

Fig. 10. The performance index J_k of the system (77).

C1: The proposed AILC method. the desired error trajectory and the transition trajectory are given as (8) and (23) in the section III, respectively. The adaptive fuzzy iterative learning controller and update laws are given as (35)-(37), respectively. The parameters are set as $c_1 = 70$, $\lambda_1 = 0.8$, $\gamma_1 = 0.6$, $\beta_1 = 0.1$, $\gamma_2 = 0.9$ and $\beta_2 = 40$. The active function in the FLSs is given as $\psi(\bar{X}_{1,k}) = e^{-(\bar{X}_{1,k}-L_j)^2/20}$, and $L = [4, 3, 2, 1, 0, -1, -2, -3, -4]^T$. The asymmetric constraint of $z_{1,k}$ is chosen as $\overline{k}_c = 0.9$, $\underline{k}_c = -1.1$.

C2: The AILC method with the rectifying action in [14]. The rectified reference trajectory is given as (69), the controller and the update law are designed as (71) and (72). The parameters in (71) and (72) are the same as those in C1 method.

The experimental results for the PMSM servo system under C1 and C2 methods are provided in Figs. 7-10 after 15th iterations. Fig. 7 shows the tracking performance of the angular position θ_k under two methods. Under the proposed C1 method, the angular position θ_k converges faster, and θ_k is guaranteed to avoid violating the asymmetric constraints over the interval $t \in [0, T]$. The control inputs are shown in Fig. 8, which is constrained. Fig. 9 indicates the error tracking performances of $e_{1,15}$, $e_{2,15}$. From Figs. 9 and 10, the performance index reduces to a quite small region with the increase of iteration. Especially, the error convergence under the method of C1 is faster and more accurate.

In summary, from the Figs. 2-10, the proposed method can achieve a satisfactory tracking performance for constrained nonparametric systems performing iteration-varying reference trajectory with arbitrary initial state errors and unknown control gain. It can relax the identical initial condition and iteration-invariance restriction with less computational cost than the constructions of rectified reference trajectories. The system output $x_{1,k}$ is guaranteed to be constrained within the asymmetric constraints in the interval $t \in [0, T]$ by the constructed asymmetric integral fractional barrier Lyapunov function, which is the same as the stability analysis.

VII. Conclusion

This paper developed an adaptive fuzzy iterative learning control method to address the state tracking issue of constrained systems with arbitrary initial state errors and unknown control gain. A novel desired error trajectory was systematically developed in the polynomial form without any assumption of the initial state values. It can also cope with the iteration-invariance restriction on the reference trajectory due to the independence of the reference trajectories. An asymmetric integral fractional barrier Lyapunov function can keep the tracking error within the preassigned boundary. Moreover, there was no need to estimate the unknown control gain function in the controller design, reducing computational burden. The future work includes investigating the design and application of adaptive iterative learning control under full state constraints.

References

[1] S. Arimoto, "Learning control theory for robotic motion," *Int. J. Adapt. Control Signal Process.*, vol. 4, no. 6, pp. 543–564, Nov. 1990.

[2] R. Chi, H. Li, N. Lin, and B. Huang, "Data-driven indirect iterative learning control," *IEEE Trans. Cybern.*, vol. 54, no. 3, pp. 1650–1660, Mar. 2024.

[3] M. Zhou, T. Li, C. Zhang, Y. Yu, X. Zhang, and C.-Y. Su, "Sliding mode iterative learning control with iteration-dependent parameter learning mechanism for nonlinear systems and its application," *IEEE Trans. Autom. Sci. Eng.*, early access, Oct. 30, 2023, doi: 10.1109/TASE.2023.3336933.

[4] C. Wang and D. Meng, "Data-based optimization control for learning systems," *IEEE Trans. Circuits Syst. II, Exp. Briefs*, vol. 70, no. 7, pp. 2560–2564, Jul. 2023.

[5] J.-X. Xu and Y. Tan, "A composite energy function-based learning control approach for nonlinear systems with time-varying parametric uncertainties," *IEEE Trans. Autom. Control*, vol. 47, no. 11, pp. 1940–1945, Nov. 2002.

[6] M. Sun, "A barbalat-like lemma with its application to learning control," *IEEE Trans. Autom. Control*, vol. 54, no. 9, pp. 2222–2225, Sep. 2009.

[7] C. Yin, J.-X. Xu, and Z. Hou, "A high-order internal model based iterative learning control scheme for nonlinear systems with time-iteration-varying parameters," *IEEE Trans. Autom. Control*, vol. 55, no. 11, pp. 2665–2670, Nov. 2010.

[8] Y. Chen, D. Huang, Y. Li, and X. Feng, "A novel iterative learning approach for tracking control of high-speed trains subject to unknown time-varying delay," *IEEE Trans. Autom. Sci. Eng.*, vol. 19, no. 1, pp. 113–121, Jan. 2022.

[9] X. Xing, K. Maqsood, D. Huang, C. Yang, and Y. Li, "Iterative learning-based robotic controller with prescribed human–robot interaction force," *IEEE Trans. Autom. Sci. Eng.*, vol. 19, no. 4, pp. 3395–3408, Oct. 2022.

[10] X. Li, D. Shen, and J.-X. Xu, "Adaptive iterative learning control for MIMO nonlinear systems performing iteration-varying tasks," *J. Franklin Inst.*, vol. 356, no. 16, pp. 9206–9231, Nov. 2019.

[11] C.-L. Zhang and J.-M. Li, "Adaptive iterative learning control of non-uniform trajectory tracking for strict feedback nonlinear time-varying systems with unknown control direction," *Appl. Math. Model.*, vol. 39, nos. 10–11, pp. 2942–2950, Jun. 2015.

[12] C.-J. Chien, "A combined adaptive law for fuzzy iterative learning control of nonlinear systems with varying control tasks," *IEEE Trans. Fuzzy Syst.*, vol. 16, no. 1, pp. 40–51, Feb. 2008.

[13] C. Zhang and J. Li, "Adaptive iterative learning control for nonlinear pure-feedback systems with initial state error based on fuzzy approximation," *J. Franklin Inst.*, vol. 351, no. 3, pp. 1483–1500, Mar. 2014.

[14] J.-X. Xu and R. Yan, "On initial conditions in iterative learning control," *IEEE Trans. Autom. Control*, vol. 50, no. 9, pp. 1349–1354, Sep. 2005.

[15] X.-D. Li, T. W. S. Chow, and L. L. Cheng, "Adaptive iterative learning control of non-linear MIMO continuous systems with iteration-varying initial error and reference trajectory," *Int. J. Syst. Sci.*, vol. 44, no. 4, pp. 786–794, Apr. 2013.

[16] M. Shen, X. Wu, J. H. Park, Y. Yi, and Y. Sun, "Iterative learning control of constrained systems with varying trial lengths under alignment condition," *IEEE Trans. Neural Netw. Learn. Syst.*, vol. 34, no. 9, pp. 6670–6676, Sep. 2023.

[17] J. Chen, J. Xie, J. Li, and W. Chen, "Human-in-the-loop fuzzy iterative learning control of consensus for unknown mixed-order nonlinear multi-agent systems," *IEEE Trans. Fuzzy Syst.*, vol. 32, no. 1, pp. 255–265, Jan. 2024.

[18] M.-X. Sun and Q.-Z. Yan, "Error tracking of iterative learning control systems," *Acta Automatica Sinica*, vol. 39, no. 3, pp. 251–262, Mar. 2013.

[19] M. Sun, T. Wu, L. Chen, and G. Zhang, "Neural AILC for error tracking against arbitrary initial shifts," *IEEE Trans. Neural Netw. Learn. Syst.*, vol. 29, no. 7, pp. 2705–2716, Jul. 2018.

[20] Q. Chen, H. Shi, and M. Sun, "Echo state network-based backstepping adaptive iterative learning control for strict-feedback systems: An error-tracking approach," *IEEE Trans. Cybern.*, vol. 50, no. 7, pp. 3009–3022, Jul. 2020.

[21] H. Shi, Q. Chen, Y. Li, and X. He, "Backstepping based adaptive iterative learning control for non-strict feedback systems with unknown input nonlinearities," *Int. J. Adapt. Control Signal Process.*, vol. 38, no. 7, pp. 2385–2403, Apr. 2024.

[22] S. Xie, Q. Chen, and Q. Yang, "Adaptive fuzzy predefined-time dynamic surface control for attitude tracking of spacecraft with state constraints," *IEEE Trans. Fuzzy Syst.*, vol. 31, no. 7, pp. 2292–2304, Jul. 2023.

[23] Q. Zhu and H. Wang, "Output feedback stabilization of stochastic feedforward systems with unknown control coefficients and unknown output function," *Automatica*, vol. 87, pp. 166–175, Jan. 2018.

[24] Q. Chen, Y. Li, Y. Hong, and H. Shi, "Prescribed-time robust repetitive learning control for PMSM servo systems," *IEEE Trans. Ind. Electron.*, early access, Feb. 27, 2024, doi: 10.1109/TIE.2024.3363757.

[25] H. Wang, M. Chen, and X. Liu, "Fuzzy adaptive fixed-time quantized feedback control for a class of nonlinear systems," *Acta Automatica Sinica*, vol. 47, no. 12, pp. 2823–2830, Dec. 2021.

[26] S. Hu, Q. Chen, X. Ren, and S. Wang, "Adaptive predefined-time synchronization and tracking control for multimotor driving servo systems," *IEEE/ASME Trans. Mechatronics*, early access, May 22, 2024, doi: 10.1109/TMECH.2024.3398695.

[27] H. Wang and Q. Zhu, "Adaptive output feedback control of stochastic nonholonomic systems with nonlinear parameterization," *Automatica*, vol. 98, pp. 247–255, Dec. 2018.

[28] S. Xie and Q. Chen, "Predefined-time disturbance estimation and attitude control for rigid spacecraft," *IEEE Trans. Circuits Syst. II, Exp. Briefs*, vol. 71, no. 4, pp. 2089–2093, Apr. 2024.

[29] Z. Zhu and Q. Zhu, "Adaptive fuzzy decentralized control for stochastic nonlinear interconnected system with nontriangular structural dynamic uncertainties," *IEEE Trans. Fuzzy Syst.*, vol. 31, no. 8, pp. 2593–2604, Aug. 2023.

[30] K. Xu, H. Wang, and P. X. Liu, "Adaptive fixed-time control for high-order stochastic nonlinear time-delay systems: An improved Lyapunov–Krasovskii function," *IEEE Trans. Cybern.*, vol. 54, no. 2, pp. 776–786, Feb. 2024.

[31] T. Zhang, M. Xia, and Y. Yi, "Adaptive neural dynamic surface control of strict-feedback nonlinear systems with full state constraints and unmodeled dynamics," *Automatica*, vol. 81, pp. 232–239, Jul. 2017.

[32] H. He, J. Na, J. Wu, Y. Huang, and Y. Xing, "Fixed-time adaptive parameter estimation for Hammerstein systems subject to dead-zone," *IEEE Trans. Ind. Electron.*, vol. 71, no. 4, pp. 3862–3872, Apr. 2024.

[33] M. Chen, G. Tao, and B. Jiang, "Dynamic surface control using neural networks for a class of uncertain nonlinear systems with input saturation," *IEEE Trans. Neural Netw. Learn. Syst.*, vol. 26, no. 9, pp. 2086–2097, Sep. 2015.

[34] Z. Zhu and Q. Zhu, "Adaptive event-triggered fuzzy control for stochastic highly nonlinear systems with time delay and nontriangular structure interconnections," *IEEE Trans. Fuzzy Syst.*, vol. 32, no. 1, pp. 27–37, Jan. 2024.

[35] J. Zheng and Z. Hou, "Model free adaptive iterative learning control based fault-tolerant control for subway train with speed sensor fault and over-speed protection," *IEEE Trans. Autom. Sci. Eng.*, vol. 21, no. 1, pp. 168–180, Jan. 2024.

[36] L. Liu, A. Chen, and Y.-J. Liu, "Adaptive fuzzy output-feedback control for switched uncertain nonlinear systems with full-state constraints," *IEEE Trans. Cybern.*, vol. 52, no. 8, pp. 7340–7351, Aug. 2022.

[37] Q. Yu and Z. Hou, "Adaptive fuzzy iterative learning control for high-speed trains with both randomly varying operation lengths and system constraints," *IEEE Trans. Fuzzy Syst.*, vol. 29, no. 8, pp. 2408–2418, Aug. 2021.

[38] K. Zhao, Y. Song, C. L. P. Chen, and L. Chen, "Adaptive asymptotic tracking with global performance for nonlinear systems with unknown control directions," *IEEE Trans. Autom. Control*, vol. 67, no. 3, pp. 1566–1573, Mar. 2022.

[39] S. Wang, H. Yu, J. Yu, J. Na, and X. Ren, "Neural-network-based adaptive funnel control for servo mechanisms with unknown dead-zone," *IEEE Trans. Cybern.*, vol. 50, no. 4, pp. 1383–1394, Apr. 2020.

[40] T.-T. Yang and J. Dong, "Adaptive asymptotic tracking funnel constraint control for high-power nonlinear multi-agent systems with non-affine nonlinear faults and fixed-time convergence," *IEEE Trans. Autom. Sci. Eng.*, early access, Nov. 24, 2023, doi: 10.1109/TASE.2023.3334721.

[41] X. Bu, B. Jiang, and H. Lei, "Nonfragile quantitative prescribed performance control of waverider vehicles with actuator saturation," *IEEE Trans. Aerosp. Electron. Syst.*, vol. 58, no. 4, pp. 3538–3548, Aug. 2022.

[42] Y. Hu, Y. Geng, B. Wu, and D. Wang, "Model-free prescribed performance control for spacecraft attitude tracking," *IEEE Trans. Control Syst. Technol.*, vol. 29, no. 1, pp. 165–179, Jan. 2021.

[43] X. Bu and H. Lei, "Fixed-time prescribed performance unknown direction control of discrete-time non-affine systems without nussbaum-type function," *IEEE Trans. Autom. Sci. Eng.*, early access, Dec. 1, 2023, doi: 10.1109/TASE.2023.3336976.

[44] X. Bu, B. Jiang, and H. Lei, "Low-complexity fuzzy neural control of constrained waverider vehicles via fragility-free prescribed performance approach," *IEEE Trans. Fuzzy Syst.*, vol. 31, no. 7, pp. 2127–2139, Jul. 2023.

[45] Y.-J. Liu, J. Li, S. Tong, and C. L. P. Chen, "Neural network control-based adaptive learning design for nonlinear systems with full-state constraints," *IEEE Trans. Neural Netw. Learn. Syst.*, vol. 27, no. 7, pp. 1562–1571, Jul. 2016.

[46] L. Liu, Y.-J. Liu, S. Tong, and Z. Gao, "Relative threshold-based event-triggered control for nonlinear constrained systems with application to aircraft wing rock motion," *IEEE Trans. Ind. Informat.*, vol. 18, no. 2, pp. 911–921, Feb. 2022.

[47] J. Wang, R. Li, G. Zhang, P. Wang, and S. Guo, "Continuous sliding mode iterative learning control for output constrained MIMO nonlinear systems," *Inf. Sci.*, vol. 556, pp. 288–304, May 2021.

[48] L. Ma and L. Liu, "Adaptive neural network control design for uncertain nonstrict feedback nonlinear system with state constraints," *IEEE Trans. Syst., Man, Cybern., Syst.*, vol. 51, no. 6, pp. 3678–3686, Jun. 2021.

[49] H. Ma, Q. Zhou, H. Li, and R. Lu, "Adaptive prescribed performance control of a flexible-joint robotic manipulator with dynamic uncertainties," *IEEE Trans. Cybern.*, vol. 52, no. 12, pp. 12905–12915, Dec. 2022.

[50] J.-X. Xu and X. Jin, "State-constrained iterative learning control for a class of MIMO systems," *IEEE Trans. Autom. Control*, vol. 58, no. 5, pp. 1322–1327, May 2013.

[51] X. Jin and Z. Hu, "Attacker-resilient adaptive path following of a quadrotor with environment-aware dynamic constraints," *IEEE Trans. Aerosp. Electron. Syst.*, vol. 59, no. 6, pp. 7822–7834, Dec. 2023.

[52] K. P. Tee, S. S. Ge, and E. H. Tay, "Barrier Lyapunov functions for the control of output-constrained nonlinear systems," *Automatica*, vol. 45, no. 4, pp. 918–927, Apr. 2009.

[53] Y.-J. Liu and S. Tong, "Barrier Lyapunov functions for Nussbaum gain adaptive control of full state constrained nonlinear systems," *Automatica*, vol. 76, pp. 143–152, Feb. 2017.

[54] Y. Liu, Y. Mei, H. Cai, C. He, T. Liu, and G. Hu, "Asymmetric input–output constraint control of a flexible variable-length rotary crane arm," *IEEE Trans. Cybern.*, vol. 52, no. 10, pp. 10582–10591, Oct. 2022.

[55] X. Jin, S.-L. Dai, and J. Liang, "Adaptive constrained formation-tracking control for a tractor-trailer mobile robot team with multiple constraints," *IEEE Trans. Autom. Control*, vol. 68, no. 3, pp. 1700–1707, Mar. 2023.

[56] X. Jin, "Nonrepetitive trajectory tracking for nonlinear autonomous agents with asymmetric output constraints using parametric iterative learning control," *Int. J. Robust Nonlinear Control*, vol. 29, no. 6, pp. 1941–1955, Apr. 2019.

[57] S. Tong, Y. Li, and S. Sui, "Adaptive fuzzy tracking control design for SISO uncertain nonstrict feedback nonlinear systems," *IEEE Trans. Fuzzy Syst.*, vol. 24, no. 6, pp. 1441–1454, Dec. 2016.

[58] J. Na, H. He, Y. Huang, and R. Dong, "Adaptive estimation of asymmetric dead-zone parameters for sandwich systems," *IEEE Trans. Control Syst. Technol.*, vol. 30, no. 3, pp. 1336–1344, May 2022.

Huihui Shi received the B.E. degree in electronic engineering and automation from the Jianxing Honors College, Zhejiang University of Technology, Hangzhou, China, in 2016, and the Ph.D. degree in control science and engineering from the College of Information Engineering, Zhejiang University of Technology, in 2023.

She is currently a Post-Doctoral Researcher with Zhejiang University of Technology. Her research interests include adaptive control and iterative learning control.

Qiang Chen (Member, IEEE) received the B.S. degree in measure and control technology and instrumentation from Hebei Agricultural University, Baoding, China, in 2006, and the Ph.D. degree in control science and engineering from Beijing Institute of Technology, Beijing, China, in 2012.

Since 2012, he has been with the College of Information Engineering, Zhejiang University of Technology, Hangzhou, China, where he was a Professor in 2022. He has published over 100 peer-reviewed papers in journals and conference proceedings. He has been authorized more than 60 invention patents, 13 of which were transferred. His research interests include adaptive control and iterative learning control with application to motion control systems.

Yihuang Hong received the B.Eng. degree in electrical engineering and automation from North University of China, Taiyuan, China, in 2021. He is currently pursuing the master's degree with the College of Information Engineering, Zhejiang University of Technology, Hangzhou, China.

His current research interests include iterative learning control theory and repetitive learning control.

Xianhua Ou (Member, IEEE) received the M.S. degree in control engineering and the Ph.D. degree in control science and engineering from the College of Information, Zhejiang University of Technology, Hangzhou, China, in 2015 and 2019, respectively.

He held a post-doctoral position with Nanyang Technological University from 2019 to 2020. He joined Zhejiang University of Technology in 2020, where he has been an Assistant Professor with the College of Information Engineering. His research interests include data-driven control and liquid desiccant dehumidification.

Xiongxiong He received the M.S. degree in operation and control from Qufu Normal University, Qufu, China, in 1994, and the Ph.D. degree in control science and engineering from Zhejiang University, Hangzhou, China, in 1997.

He held a post-doctoral position with Harbin Institute of Technology from 1998 to 2000. He joined Zhejiang University of Technology in 2001, where he has been a Professor with the College of Information Engineering.